Comparison of analytic and numerical results for the mean cluster density in continuum percolation

James A. Given
Department of Chemistry, SUNY Stony Brook, Stony Brook, New York 11794

In Chan Kim
Department of Mechanical and Aerospace Engineering, North Carolina State University, Raleigh, North Carolina 27695-7910

S. Torquato
Department of Mechanical and Aerospace Engineering and Department of Chemical Engineering, North Carolina State University, Raleigh, North Carolina 27695-7910

George Stell
Department of Chemistry, SUNY Stony Brook, Stony Brook, New York 11794

(Received 5 April 1990; accepted 27 June 1990)

Recently a number of techniques have been developed for bounding and approximating the important quantities in a description of continuum percolation models, such as $\langle n_c \rangle / \overline{\rho}$, the mean number of clusters per particle. These techniques include Kirkwood–Salsburg bounds, and approximations from cluster enumeration series of Mayer–Montroll type, and the scaled-particle theory of percolation. In this paper, we test all of these bounds and approximations numerically by conducting the first systematic simulations of $\langle n_c \rangle / \overline{\rho}$ for continuum percolation. The rigorous Kirkwood–Salsburg bounds are confirmed numerically in both two and three dimensions. Although this class of bounds seems not to converge rapidly for higher densities, averaging an upper bound with the corresponding lower bound gives an exceptionally good estimate at all densities. The scaled-particle theory of percolation is shown to give extremely good estimates for the density of clusters in both two and three dimensions at all densities below the percolation threshold. Also, partial sums of the virial series for $\langle n_c \rangle$ are shown numerically to give extremely tight upper and lower bounds for this quantity. We argue that these partial sums may have similar bounding properties for a general class of percolation models.

I. INTRODUCTION

The basic concept of percolation as a geometrical effect underlying nucleation and aggregation processes has been used by researchers for several decades.[1–17] In general, it involves the creation of large clusters of atoms or particles by a process of pairwise aggregation or "connection." The fact that a smooth change either in the density of particles or in the definition of pairwise connectedness can produce a sudden change in the average size of the resultant clusters is well known; the resulting, purely geometrical transition is called the "percolation transition."

This phenomenon is very general. The particles' positions may either be correlated according to an arbitrary thermal Gibbs distribution function or according to some nonequilibrium deposition process. In a continuum system, the condition under which a pair of particles are taken to be connected can be chosen in many ways, depending on the application; it need have no relation to the correlation between the particle positions. For example, in studying impurity conduction in a crystal,[10] it is natural to choose a separation-dependent bond probability proportional to $\exp[-x_{ij}/\xi]$; here x_{ij} is the separation and ξ is the hopping length.

Recently, the extensive study of the percolation critical indices with their attendant universality has caused researchers to focus on uncorrelated, nearest-neighbor percolation on a lattice. This paper is part of a long-term effort to develop techniques for studying percolation processes in the generality indicated above.

Hill[6] first provided a general framework for calculating percolation quantities by writing the thermal Mayer function for a system as a sum of "connecting" and "blocking" Mayer functions, substituting for each bond in the thermal Mayer graph series, expanding and retaining only subgraphs with a path of connecting bonds joining the root points. This procedure has allowed the development of both series expansions[2,3,11] and integral equations [4,5,13,14] for the basic quantities of interest in a variety of correlated percolation models.

This method was applied by Coniglio *et al.*[2] to give series expansion methods for continuum percolation quantities. Recently the continuum Potts model (CPM) method[12–14] has been used[15] to derive such expressions, as well as other relations which are new. This method extends to the continuum the Potts model mapping of Fortuin and Kastelyn[7] which yields percolation models as a limiting form of thermal model. It allows one to automatically select the terms given by Hill's prescription; thus it is a convenient way to develop equations for percolation quantities. The CPM method treats percolation as the one-state limit of a standard continuum statistical mechanical system, thus, it is straightforward to use this method to derive

 0021-9606/90/195128-12$03.00

analogs for percolation of the series expansions and integral equations already available from the theory of liquids.

In this paper, we evaluate several approximations and bounds for the quantity $\langle n_c \rangle$, the mean number of clusters per unit volume, which have been derived by using the CPM approach. These include a Kirkwood–Salsburg equation for $\langle n_c \rangle$,[14] which produces a sequence of increasingly accurate upper and lower bounds for this quantity, and a number of approximations for $\langle n_c \rangle$ from the scaled particle theory of percolation.[15]

To evaluate this wealth of analytic expressions, we conducted the first extensive computer simulations of the total cluster density per particle in continuum percolation. Estimates of the density of small clusters of fixed size have previously been obtained.[8] However, our purpose was to appraise the functional dependence of the quantity $\langle n_c \rangle$ on particle density, and thus we required somewhat more extensive simulations than those done previously.

Obtaining statistical measures such as mean numbers of clusters, monomers, dimers, and trimers, etc., from computer simulations is a two-step process. First, one generates realizations of the random medium. Second, one samples each realization for the desired quantities and then averages over a sufficiently large number of realizations. We generated realizations of random sphere percolation (i.e., distributions of points with a Poisson distribution) by randomly placing particles in a D-dimensional cubical cell. The cell is surrounded by periodic images of itself. The advantages of "free" boundary conditions over standard periodic boundary condition in obtaining the connectedness functions by simulations have been described previously.[16] It will not make any difference in the determination of cluster statistics, however. Sampling each realization to calculate the mean number of clusters, monomers, dimers, and trimers was done by a modified Hoshen–Kopelman[17] cluster labeling algorithm. We first computed these quantities for several system sizes (i.e., number of particles in the cell for some fixed density) and then extrapolated the results to the infinite-size limit. We have studied systems of 60, 120, 250, 500, and 1000 particles in two dimensions and systems of 64, 125, 216, 512, and 1000 particles in three dimensions. We generated sets of 3000 realizations in two dimensions and sets of 4500–5000 realizations in three dimensions.

This paper is organized as follows: in Sec. II, the derivation of the Kirkwood–Salsburg hierarchy for percolation is sketched. The first equation in this hierarchy is then used to give various upper and lower bounds for $\langle n_c \rangle$. In Sec. III, a class of approximations from the scaled particle theory of percolation are developed and compared with simulation data. In Sec. IV, we develop a Mayer–Montroll hierarchy for the percolation cluster numbers $n_c(k)$. These give the mean number per unit volume of clusters containing k particles. Truncations of this hierarchy are shown to give good approximations for the quantities $n_c(k)$, whose sum is the mean density of clusters $\langle n_c \rangle$. In Sec. V, we develop lower bounds on $\langle n_c \rangle$ by enumerating the number of monomers, dimers, and trimers per unit volume. These enumeration bounds are compared to simulation data. Section VI gives our conclusions. Also included are three technical appendices: Appendix A gives geometric formulas basic to the enumeration of dimers and trimers, Appendix B gives the fourth-order bounds of Kirkwood–Salsburg type on mean cluster number, and Appendix C uses the scaled particle theory of percolation to derive a differential equation for the mean cluster number.

II. KIRKWOOD–SALSBURG BOUNDS FOR PERCOLATION

In this section, we sketch the derivation of a Kirkwood–Salsburg hierarchy for the n-point connectedness functions which was given in detail in Ref. 14. Truncations of the equations in this hierarchy give alternately upper and lower bounds on the connectedness functions. Since the first equation in this hierarchy is satisfied by the density derivative of $\langle n_c \rangle$, bounds on this quantity are also obtained.

A word about our choice of units is necessary. Although we find it aids intuition to develop our equations in terms of the number density of particles $\overline{\rho}$, all our graphs use the reduced density η. This is defined as the number density times the particle volume. Thus one has $\eta = (\pi/4)a^2\overline{\rho}$ and $\eta = (\pi/6)a^3\overline{\rho}$ in two and three dimensions, respectively. The length a is both the particle diameter and the characteristic range of the bond probability, to be defined below.

The Kirkwood–Salsburg (KS) hierarchy for random percolation[14] shares certain basic features with the corresponding hierarchy for repulsive thermal interactions,[22] although its structure is substantially more complex. Because of this, the hierarchy has been used to develop rigorous upper and lower bounds for the basic quantities of percolation theory, as well as to provide a lower bound for the radius of convergence of the virial series. The KS hierarchy is most readily developed by exploiting the relation between the continuum Potts model (CPM) and continuum percolation. The pairwise interaction for the continuum Potts model

$$V_{ij} = v(x_{ij})[1 - \delta_{\alpha_i\alpha_j}] + \phi(x_{ij}) \tag{2.1}$$

describes a many-body system of particles, each of which is in one of s different species or spin states, with a positive interaction $v(x)$ acting only between particles of different species. The spin-independent interaction $\phi(x)$ will induce correlations in particle positions in the corresponding percolation model. Although the methods reviewed here apply to models with general positive $\phi(x)$, it suffices for our purposes here to set $\phi(x) = 0$, as we will discuss only random percolation in this paper. The CPM can also be described as an s-species generalization of the Widom–Rowlinson model, a useful model for phase separation.[18] The one-state limits of the physical quantities describing this model are the corresponding quantities describing a continuum percolation model in which particles are randomly centered and connected with a separation-dependent bond probability $p_b(x)$. Here

$$p_b(x_{ij}) = 1 - \exp[-\beta v(x_{ij})]. \tag{2.2}$$

If $v(x)$ is chosen to be a hard-sphere interaction with diameter a, this gives the model called sphere percolation, in which two particles are connected only if their centers are closer together than a. In this paper we will compare computer simulation data from this model to a variety of analytic bounds and approximations that have been obtained previously. However, most of the methods discussed here apply with suitable extension to any percolation model that can be described as the one-state limit of the CPM defined by Eq. (2.1). As noted above, this is a large class of models.

The density ρ and fugacity z of the CPM are related to the mean number of clusters in random percolation by

$$\left.\frac{d}{ds}\right|_{s=1}\left(\frac{\rho}{z}\right)=\frac{d}{d\overline{\rho}}\langle n_c\rangle-1. \tag{2.3}$$

Here $\overline{\rho}$ and $\langle n_c\rangle$ are, respectively, the number of particles and number of clusters, per unit volume, in the corresponding percolation model. In the zero-field case to be discussed here, the thermal correlation functions of the CPM do not depend on which spin states particles occupy, but only on whether each pair of particles is in the same, or different, spin states. Thus we can write

$$g_t(1,...,n;P)\equiv g_t(x_1,\alpha_1,...,x_n,\alpha_n) \tag{2.4}$$

for the CPM thermal correlation function; it is proportional to the probability density for finding particles at positions x_1, x_2, ... ,x_n in spin states α_1, α_2, ..., α_n, respectively. We use a normalization such that $g_t\to 1$ when all the differences of pairs of spatial arguments of this function simultaneously become large. Here P is a partition of the integers 1,...,n in which two integers are grouped together if and only if the corresponding particles are in the same spin state. Note that we write 1 for x_1, 2 for x_2, etc. The corresponding objects in percolation theory, the connectedness functions, are similarly proportional to the probability densities associated with finding particles at x_1, ..., x_n connected together in various subclusters. Here, a pair of particles is said to be connected, or contained in the same cluster, if there is a chain of pairwise-connected particles liking them. This quantity is written $g_c(1,...,n;P)$, where P is a partition of integers 1,...,n in which two integers are grouped together only if the corresponding particles are to be in the same connected cluster. Since a group of n particles can be linked into clusters by the other particles in the system $n!$ possible ways, there are $n!$ connectedness functions on the n-point level. The complexity of the percolation problem is largely due to the fact that hierarchies of integral equations for these functions tend to involve the entire set. On the two-point level, there are just two functions, usually called the connectedness function $g_c(1,2)$, and the blocking function $g_c(1/2)$. These give the probability density for finding the two particles centered at x_1 and x_2, respectively, in the same cluster, and in different clusters. The connectedness functions are related to the one-state limit of the CPM correlation functions by

$$\lim_{s\to 1} g_t(1,...,n;P)=\sum_{P'<P} g_c(1,...,n;P'). \tag{2.5}$$

Here the sum is over partitions P' of the integers 1,...,n which are refinements of P.

Integral equations for various subsets of the connectedness functions have been developed and studied numerically. In general, however, percolation theory is most cleanly formulated using not the connectedness functions, but the specific linear combination of them which occurs on the right-hand side of Eq. (2.5). These functions, which we call the generalized blocking functions, are written $g_b(1,...,n;P)$. They yield the probability density for finding particles $x_1,...,x_n$, such that *no* connections exist between any pair of particles whose indices are separated by the partition P; particles whose indices are grouped together may be either connected or not. This insight, i.e., that the $s\to 1$ limit of the CPM correlation function is a useful linear combination of connectedness functions, then allows a direct relation between the CPM and continuum percolation. The Kirkwood–Salsburg hierarchy for the CPM correlation functions

$$\frac{\rho(x_1,\alpha_1)}{z}=1+\sum_{m=1}^{\infty}\frac{\rho^m}{m!}\sum_{\alpha_2}\cdots\sum_{\alpha_{m+1}}\int\prod_{k=2}^{m+1}f(x_1,x_k,\alpha_1,\alpha_k)$$

$$\otimes g_t[2\alpha_2,...,(m+1)\alpha_{m+1}]dx_2...dx_{m+1} \tag{2.6a}$$

$$g_t(1\alpha_1,...,n\alpha_n)=\left(\frac{z}{\rho}\right)\prod_{k=2}^{n}[1+f(x_{1k},\alpha_1,\alpha_k)]\Big[g_t(2\alpha_2,...,n\alpha_n)$$

$$+\sum_{m=1}^{\infty}\frac{\rho^m}{m!}\sum_{\alpha_{n+1}}\cdots\sum_{\alpha_{n+m}}\int\prod_{k=n+1}^{n+m}f(x_1,x_k,\alpha_1,\alpha_k)$$

$$\otimes g_t[2\alpha_2,...,(n+m)\alpha_{n+m}]dx_{n+1}...dx_{n+m}\Big] \tag{2.6b}$$

can be written down directly, pairing each integral over particle position with a sum over that particle's spin. If one takes the one-state limit of these equations, using Eq. (2.5), and groups together identical terms, the result is

$$g_b(1,\ldots,n;P) = \prod_{k=2}^{n} \{p_b(1,k)\delta_{\alpha_1,\alpha_k} + [1-p_b(1,k)]\}\Big[g_b(2,\ldots,n;P) + \sum_{m=1}^{\infty} \frac{(-\overline{\rho})^m}{m!} \sum_{P'} d(P,P') \int \prod_{k=n+1}^{n+m} p_b(1,k) \otimes g_b(2,\ldots,n+m;P')dx_{n+1}\ldots dx_{n+m}\Big]. \quad (2.7)$$

Here P is a partition of $1,\ldots,n$, P' is a partition of $2,\ldots,n+m$, and the second sum on the right-hand side is over partitions P' that are consistent with P, i.e., that agree with P when restricted to the integers $2,\ldots,n$. The weight factor $d(P,P')$ depends on the structure of these two partitions and can be calculated in closed form.[14] In order to use this hierarchy to derive various bounds pertaining to $\langle n_c\rangle$, an equation for this quantity must be added to the hierarchy. To do this, we take an s derivative of both sides of Eq. (2.6a) and use the relation (2.3). This gives an equation for the density derivative of $\langle n_c\rangle$ of the form (2.7), but with a different form for the weight factors:

$$\frac{d}{d\overline{\rho}}\langle n_c\rangle = 1 + \sum_{m=1}^{\infty} \frac{(-\overline{\rho})^m}{m!} \sum_{p'} \overline{d}(p') \int \prod_{k=2}^{m+1} p_b(x_{1k}) \times g_c(2,\ldots,m+1)dx_2\ldots dx_{m+1}. \quad (2.8)$$

Note that Eq. (2.8) is said to have the same form as Eq. (2.7), and to belong to the same hierarchy, because the $\{g_c\}$ and the $\{g_b\}$ form equivalent bases, i.e., either set of functions contains a full description of the cluster structure of a percolation model. Equation (2.8) is needed in order to include $\langle n_c\rangle$ in a closed set of equations that have the properties needed to develop analytic bounds.

This hierarchy now allows the derivation of powerful, exact results. Because the bond probability is positive, i.e., because we chose $v(x)$ in Eq. (2.1) to be greater than zero, the hierarchy inherits the alternating bound property from the corresponding thermal CPM hierarchy[22]; i.e., successive truncations of any of Eqs. (2.7) will give alternating upper and lower bounds for the blocking functions. Since these form a complete set, one can substitute these bounds into each other, eliminating the blocking functions on the right-hand side and finally yielding bounds on these functions that depend only on $p_b(x)$ and the density $\overline{\rho}$. Again, because the connectedness functions are linear combinations of the blocking functions, [see Eq. (2.5)], one gets the desired bounds on these quantities. Since $\langle n_c\rangle$ was included in the hierarchy, we obtain bounds for it as well. Some low-order bounds obtained in this manner are

$$\langle n_c\rangle \geqslant \overline{\rho} - \tfrac{1}{2}\overline{\rho}^2 A_2, \quad (2.9)$$

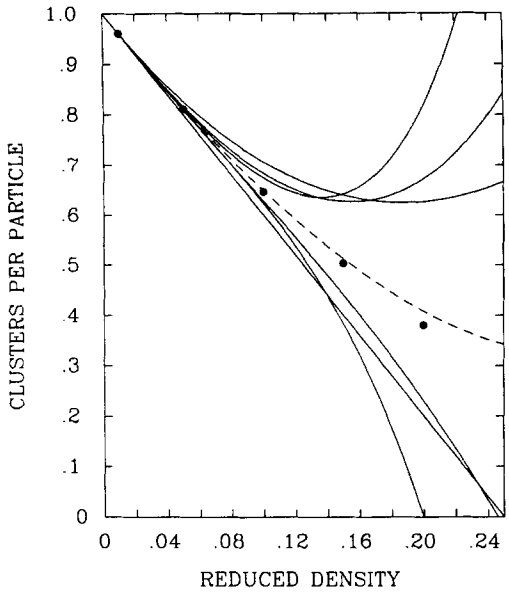

FIG. 1. Three upper and three lower bounds on the 3D cluster density $\langle n_c\rangle/\overline{\rho}$, shown as solid curves. These result from the Kirkwood–Salsburg bounds described in Sec. II, after successive substitution to eliminate blocking functions [see Eqs. (2.8)–(2.11) and also Appendix B]. For low densities, successive bounds improve; for higher densities this is not the case. The average of fourth-order lower and upper bounds, shown as a dotted curve, gives a very good approximation to the simulation data points, shown as solid circles.

$$\langle n_c\rangle \leqslant \overline{\rho} - \tfrac{1}{2}\overline{\rho}^2 A_2 + \tfrac{1}{6}\overline{\rho}^3 A_2^2, \quad (2.10)$$

$$\langle n_c\rangle \geqslant \overline{\rho} - \tfrac{1}{2}\overline{\rho}^2 A_2 + \tfrac{1}{6}\overline{\rho}^3 A_3 - \tfrac{1}{24}\overline{\rho}^4 A_2^3, \quad (2.11)$$

$$\langle n_c\rangle \leqslant \overline{\rho} - \tfrac{1}{2}\overline{\rho}^2 A_2 + \tfrac{1}{6}A_3\overline{\rho}^3 + \tfrac{1}{8}\overline{\rho}^4 A_2^*[A_2^2 - A_3], \quad (2.12)$$

where

$$A_2 = \int d^3x_{12} p_b(x_{12}) \quad (2.13)$$

$$A_3 = \int d^3x_{12}\, d^3x_{23}\, p_b(x_{12})p_b(x_{23})p_b(x_{31}). \quad (2.14)$$

We also calculated the fourth-order bounds in this sequence; these are given in detail in Appendix B. All of these bounds are graphed and compared with computer simulation data in Fig. 1. For low densities, the upper and lower bounds closely bracket the simulation results. However, for intermediate densities, where this is not true, none of the bounds give a close approximation to the data. In this regard, these bounds for random percolation differ from the variational bounds[26] on the transport properties of random systems. It is frequently the case with the latter that either the upper or the lower bound will closely approximate the data. It is entirely possible that bounds for strongly correlated percolation models may behave differently in this regard, but this matter is still unexplored. We note, however, that for the case of random percolation explored here, the averages of successive pairs of upper and lower bounds give remarkably good approximations to the simulation data. As an example, the average of the upper

and lower bound of fourth order given by the procedure described above is shown as a dashed line in Fig. 1. Also, we note that the higher-order bounds do increasingly well at low densities but actually deviate from the data more rapidly at higher density. This seems to represent the cumulative effect on the remainder term of successive substitutions. Support for this view is given in the discussion of the bound (2.19). Bounds of the type discussed in this section exist for percolation models with positive (repulsive) correlating potentials $\phi(x)$, although their functional form is somewhat more complicated.[14]

The two-point connectedness function is bounded by

$$g_c(x_1,x_2) \geqslant p_b(x_{12}), \tag{2.15}$$

$$g_c(x_1,x_2) \leqslant p_b(x_{12}) + [1 - p_b(x_{12})]\,\overline{\rho}\,A_2. \tag{2.16}$$

These bounds yield corresponding bounds for the cluster density $\langle n_c \rangle$ if they are inserted into the right-hand side of the virial theorem for sphere percolation. This relation is[11]

$$\frac{d}{d\overline{\rho}}\left(\frac{\langle n_c\rangle}{\overline{\rho}}\right) = -\frac{1}{2}\left(\frac{4}{3}\pi a^3\right) g_b(a,\overline{\rho}\,). \tag{2.17}$$

Thus, if the quantity on the right-hand side is known, it can be immediately integrated to give $\langle n_c \rangle$. For sphere percolation, one can exploit the fact that quantities depend only on the dimensionless combination $\overline{\rho}a^3$ to rewrite Eq. (2.17),

$$\frac{d}{da}\left(\frac{\langle n_c\rangle}{\overline{\rho}}\right) = -\frac{1}{2}\,(4\pi a^2) g_b(a,\overline{\rho}\,). \tag{2.18}$$

This equation has a simple probabilistic interpretation: if the radius of every particle in a realization of sphere percolation is increased by an amount da, the decrease in the number of clusters per particle is given by the density, at the surface of one particle, of particles belonging to different clusters. Each of these corresponds to an incipient fusion of two clusters. The factor of 1/2 on the right-hand side of Eq. (2.18) prevents double counting. A relation of this kind can be developed for any continuum percolation model with a positive (repulsive) correlating potential $\phi(x)$.

No simple relation pertains between the low-order bounds on $\langle n_c \rangle$ developed directly from the Kirkwood–Salsburg equation and those developed by using Eq. (2.17). Neither set of bounds is consistently tighter, at the same level of approximation. Thus it is an advantage to work with both sets.

We also investigated the Kirkwood–Salsburg upper bound on $\langle n_c \rangle$,

$$\frac{d}{d\overline{\rho}}\langle n_c\rangle \leqslant 1 - \overline{\rho}\,A_2 + \frac{\overline{\rho}^{\,2}}{2!}\int g_c(1,2)p_b(1,2)dx_{12} \tag{2.19}$$

which is the first nontrivial truncation of Eq. (2.8), by directly substituting, for the two-point connectedness function $g_c(1,2)$, the solution of the Percus–Yevick equation for this model.[5(a)] Evaluation of Eq. (2.19) is greatly simplified by rewriting the last term on the right-hand side

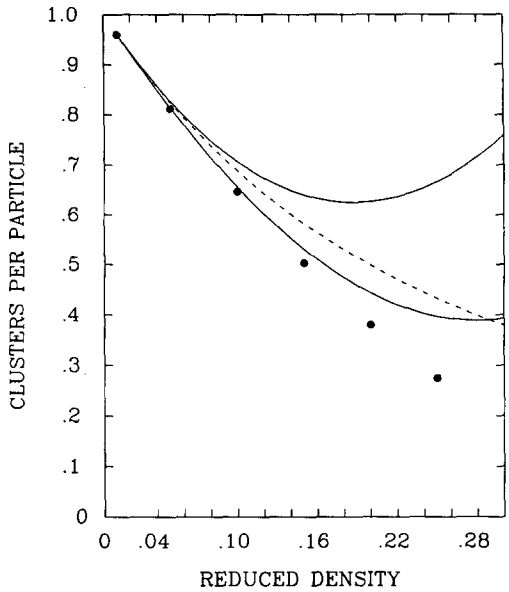

FIG. 2. The second-order Kirkwood–Salsburg upper bound (2.19) for the quantity $\langle n_c \rangle/\overline{\rho}$, evaluated by using the Percus–Yevick solution [Ref. 5(a)] for the connectedness function $g_c(x)$. This bound is a much better estimate than the corresponding truncation of the virial series, both of which are shown as solid curves. We also show as a dotted curve the resummation of the series (2.8) which follows readily if the connectedness functions in that formula are all approximated by unity (see discussion at the end of Sec. II).

$$15\eta^2 + 6\eta^2 \cdot \int_1^2 (z+4)(z-2)^2 z^2 g_c(z)dz. \tag{2.20}$$

Here we use the reduced density for 3D which is $\eta = (\pi/6)\overline{\rho}a^3$. The result is shown in Fig. 2, where it is compared to the polynomial given by the first three terms of the virial series for this quantity. Although both are exact to order $\overline{\rho}^{\,3}$, Eq. (2.19) gives a far better approximation to the actual value of $\langle n_c \rangle$ for intermediate density. This is actually the best rigorous bound we have evaluated for this quantity. Thus, it seems valuable to calculate higher-order bounds of this type by using the best approximations to two and three-point connectedness functions, as provided, for example, by integral equation studies.[5,13]

Equation (2.8) suggests one other natural approximation. For the case of sphere percolation (or any other short-range percolation model), the connectedness functions in that formula are evaluated only for small separations of their arguments. In this domain, the connectedness functions will be close to unity. Approximating them by unity allows one to sum the series on the right-hand side of Eq. (2.8) to give $\exp[-\overline{\rho}A_2] - 1$. This gives a very reasonable approximation for $\langle n_c \rangle$ which is shown by a dotted line in Fig. 2.

III. SCALED PARTICLE THEORY APPROXIMATIONS

In this section, we sketch the development of a scaled particle theory for continuum percolation models.[15] The theory is quite general, although the development here will be specified to the case of random-sphere percolation, both for brevity, and to avail ourselves of the direct probabilistic

interpretation that this model allows. We develop a general scheme for producing scaled-particle approximations to the cluster density for this model. The relative importance of the various constraint conditions will then be assessed by comparing the approximations to simulation data.

For random-sphere percolation, we define the notion of a scaled particle, or λ-cule, as follows: in a realization of this system with density $\overline{\rho}$, locate at random a point particle, considered as a sphere with zero radius. The sphere then increases steadily in radius, and as it does, it includes the centers of other particles and thus becomes connected to them. Some of these are already connected indirectly to the scaled particle, i.e., are contained in the same cluster, whereas some are not. The probability density associated with overlapping a particle from a different cluster, as the scaled particle radius increases from λ to $(\lambda + d\lambda)$ can be written

$$G(\lambda, \overline{\rho}\,) 4\pi\lambda^2\, d\lambda. \tag{3.1}$$

This defines the scaled particle function $G(\lambda,\overline{\rho})$. If the variable λ is set equal to a, the diameter of the other particles in the system, the function G becomes the contact value of the two-point blocking function. Knowledge of this quantity as a function of density is equivalent to knowledge of $\langle n_c\rangle$. This is the content of the virial theorem (2.17).

It will be valuable, in deriving relations for $G(\lambda,\overline{\rho})$, to relate this quantity to the functions already developed in Sec. II. To do this, define a generalized blocking function $g_b(x_{12},\lambda)$ as follows: $g_b(x_{12},\lambda)$ is the probability density associated with finding a normal particle and a λ-cule separated by a distance x_{12}, with the two belonging to different clusters. By the definition of $G(\lambda,\overline{\rho})$ in Eq. (3.1), we have immediately

$$G(\lambda, \overline{\rho}\,) = g_b(\lambda,\lambda). \tag{3.2}$$

The behavior of $G(\lambda,\overline{\rho})$ for small values of λ is easily determined. In fact, if a normal particle and a λ-cule are separated by a distance $\lambda \leqslant a/2$, any particle connected to the λ-cule will also be connected to the normal particle. Thus the two will fail to be connected only if the λ-cule is empty of particle centers. The probability for this is

$$G(\lambda, \overline{\rho}\,) = \exp(-\overline{\rho}\,\tfrac{4}{3}\pi\lambda^3). \tag{3.3}$$

The above comments then provide a strategy for calculating $\langle n_c\rangle$. The function $G(\lambda,\overline{\rho})$ is known for small λ, and, if additional relations can be used to interpolate it to $\lambda = a$, the virial theorem (2.17) will then give $\langle n_c\rangle$.

Other relations satisfied by $G(\lambda,\overline{\rho})$ are easily obtained. For example, one has the relation

$$\frac{d}{d\overline{\rho}}\langle n_c\rangle = 1 - \overline{\rho}\int_0^a 4\pi\lambda^2 g_b(\lambda,\lambda)\,d\lambda \tag{3.4}$$

which has been termed[15] the charging relation. This name reflects the fact that increasing the radius of a particle in a percolation model is analogous to increasing the charge, or interaction strength, of a particle in a thermal system. Equation (3.4) has a direct probabilistic interpretation, which is rather similar to that already given for the virial theorem of percolation. To see this, we examine the change in the number of clusters per unit volume produced by adding one particle to the system. The particle will be added in a specific manner: we insert at a random location a λ-cule with range $\lambda = 0$ and allow it to grow until it becomes a normal particle. As the range of the λ-cule increases from λ to $(\lambda + d\lambda)$, the probability that it overlaps a particle from a different cluster is given by

$$4\pi\lambda^2\overline{\rho}\, g_b(\lambda,\lambda)\,d\lambda. \tag{3.5}$$

The total change in the number of clusters produced by such an addition is then equal to 1 (for the λ-cule itself) minus the number of events in which the λ-cule fuses with other clusters, i.e., minus the integral of Eq. (3.5). This is the content of the charging relation (3.4). This argument also makes it clear that the charging relation (3.4), like the virial theorem (2.17), can be generalized to an arbitrary percolation model, although the derivation given above exploited the geometric nature of sphere percolation.

The relation

$$\langle n_c\rangle = \overline{\rho}\, G(\infty, \overline{\rho}\,) \tag{3.6}$$

known as the osmotic pressure relation for percolation,[15] has also been established by the use of the inclusion–exclusion argument.

More information on the function $G(\lambda,\overline{\rho})$ is available. By using a Kirkwood–Salsburg equation for $G(\lambda,\overline{\rho})$, together with geometrical information, one can calculate the value of $G(\lambda,\overline{\rho})$ and its first two derivatives at the point $\lambda = a/2$. This calculation is described in detail in Ref. 15.

As already noted, the relations given in this section can be readily derived by using the known relationships between the quantities describing the CPM and those describing continuum percolation. A scaled particle theory can be readily derived for the CPM by defining a λ-cule for that model to be a particle of a particular species (say species i) with interaction range λ. The CPM mapping is not needed for the model of random-sphere percolation, for which probability theory is sufficient to derive the necessary constraint relations. The CPM method is valuable, however, in deriving scaled particle theory for the general case of correlated percolation.

We now have a general basis for constructing scaled-particle approximations for the basic percolation quantities discussed in this work, the mean number of clusters $\langle n_c\rangle$, and the value of the blocking function at contact $\overline{g}_c(a,\overline{\rho}\,)$. It will be convenient to use the notation $y = \lambda/a$ and $t \equiv \eta$ in what follows. We retain a finite number of terms of the expansion

$$g_b(\lambda,\lambda) = \sum_{n=0}^{\infty} G_n(\overline{\rho}\,)\left(\frac{a}{\lambda}\right)^n \tag{3.7}$$

and solve for the coefficients G_n using the constraint equations mentioned above. We summarize the constraint equations to be used:

(1) The value of $G(\lambda,\overline{\rho})$ at $y = \frac{1}{2}$ given by Eq. (3.3) (F);

(2) The value of the first derivative of $G(\lambda,\overline{\rho})$ with respect to λ at $y=\frac{1}{2}$ (1D);
(3) The value of the second derivative of $G(\lambda,\overline{\rho})$ at $y=\frac{1}{2}$, taking into account the discontinuity in that quantity (2D);
(4) The charging relation for percolation Eq. (3.4) (CH);
(5) The osmotic pressure equation for percolation (3.6) (OS);
(6) The virial theorem for percolation Eq. (2.17) (VT).

Note that in an exact treatment, constraints (4), (5), and (6) would not all be independent; one of them would serve to transfer the discussion from $G(\lambda,\overline{\rho})$ to $\langle n_c\rangle$. However, in an approximate treatment, use of all three constraints does yield a better estimate, as we will see. More constraints can be included. For example, one can use the short-distance techniques already discussed, including geometrical probability theory and the Kirkwood–Salsburg equations, to calculate higher derivatives of $G(\lambda)$ at $y=\frac{1}{2}$. We do not pursue this here.

We consider in detail five approximation schemes, each resulting from the use of a subset of the above six constraint equations. These approximations and their corresponding set of constraints are

(A1) (F, 1D, 2D, CH, VT)
(A2) (F, 1D, 2D, CH, OS)
(A3) (F, 1D, 2D, VT, OS)
(A4) (F, 1D, CH, VT, OS)
(A5) (F, 1D, 2D, CH, VT, OS).

We have abbreviated each constraint as above. The second derivative fixed by constraint number (A3) can be shown to be infinite in two dimensions; thus this constraint cannot be enforced with a polynomial fit and is absent in two dimensions. We still use the same notation, however, simply identifying (A4) and (A5). We graph the resulting set of approximations for two-dimensional percolation in Fig. 3. The approximations (A5), given by the full set of constraints, and shown in the figure with a solid curve, is the best at all densities below the percolation threshold. The others, in decreasing order of accuracy, are (A1), (A2), and (A3).

The situation in three dimensions is more subtle. (See Fig. 4.) The full approximation (A5), again shown with a solid curve, is the best at all densities below $\eta = 0.27$. At higher densities, other approximations, first (A1), and then (A2), come to fit the data more closely. It is not clear without further application of this method how general this sequence is, however, it may simply reflect the limits of accuracy of the present scheme. The detailed behavior of these approximation schemes for high density is shown in Fig. 5. Note from both Figs. 4 and 5 that the three-dimensional scaled-particle estimates are more tightly clustered than the two-dimensional estimates.

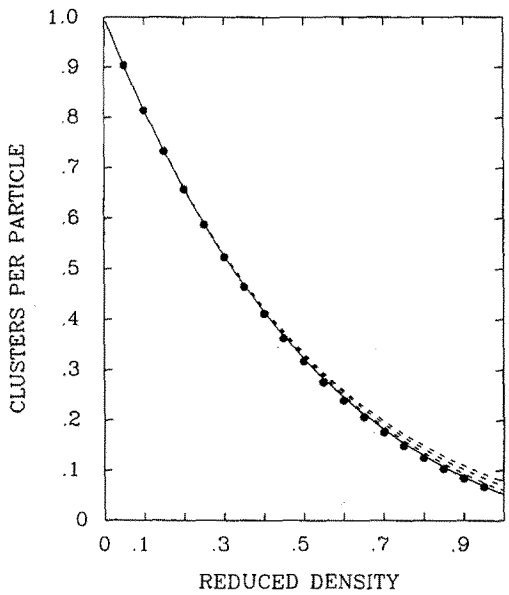

FIG. 3. Four scaled-particle approximations in 2D, vs computer simulation data for the cluster density $\langle n_c\rangle/\overline{\rho}$. These are discussed in detail below Eq. (3.7). The full approximation (A5), shown as a solid curve, is consistently the best for all densities below the percolation transition, which occurs at a reduced density $\eta = 1.15$. The others, in decreasing order of accuracy, are those termed (A1), (A2), (A3), all of which are shown as dotted curves.

IV. MAYER–MONTROLL EQUATIONS FOR CLUSTER DENSITY

In this section, we develop a Mayer–Montroll hierarchy for the density of clusters containing a specified number of particles. We explore this series numerically in the case of random-sphere percolation, both for its intrinsic interest as a source of information about the cluster size distribution, and as a way to explore the analytic structure of the virial series that occur in percolation theory.

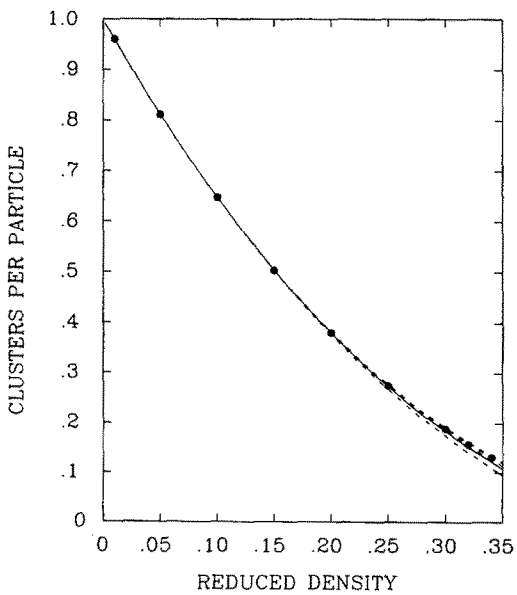

FIG. 4. Same as Fig. 3, but for 3D percolation. The full approximation (A5) is still the best below the reduced density $\eta = 0.27$. At higher densities, the approximations (A1) and (A2) best describe the data. Again, scaled-particle approximations are quite accurate up to the transition, which occurs at a density $\eta = 0.35$.

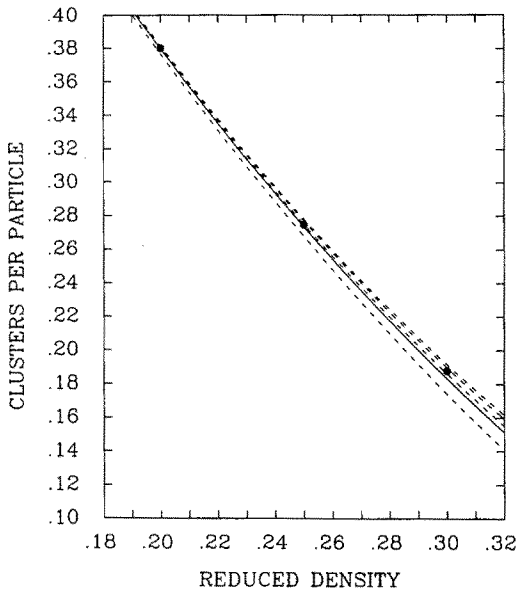

FIG. 5. Detail from Fig. 4. The approximations, shown, from bottom to top, respectively, are those termed (A4), (A5) (shown as a solid curve), (A1), (A2), and (A3). See discussion at the end of Sec. III.

Define the quantity $n_c(k,\overline{\rho})$ to be the density, per unit volume, of clusters containing exactly k particles. We first write down the Mayer–Montroll equation for the quantity $n_c(k,\overline{\rho})$, then give a probabilistic interpretation of this equation. The equation is

$$n_c(k,\overline{\rho}) = \int \rho_t(1,...,k) I_1(1,...,k) I_2(1,...,k) \times dx_1 ... dx_k. \tag{4.1}$$

The interpretation of this equation is as follows: in order for particles at $x_1,...,x_k$ to constitute a k cluster, three events must occur: there must be particles at these positions, they must be connected into a cluster without the need for intermediaries, and they must not be connected to any other particle. These correspond to the three factors in the integrand of Eq. (4.1). The first is the probability density for finding particles at positions $x_1,...,x_k$. The second is given by the sum of all connected Mayer graphs, with each pair of particles i and j weighted, either by a factor $p(x_{ij})$ or $[1-p_b(x_{ij})]$, depending on whether the points i and j are or are not connected by a line. For example, for $k=3$, one has

$$\begin{aligned} I(1,2,3) = & p_b(1,2)p_b(1,3)[1-p_b(3,1)] \\ & + \text{cyclic permutations} \\ & + p_b(1,2)p_b(2,3)p_b(3,1). \end{aligned} \tag{4.2}$$

The third factor gives the probability density associated with the event that no other particles be connected to those located at $x_1,...,x_k$. This is given by a standard Mayer–Montroll inclusion–exclusion argument.[19] The result is

$$I_2(1,...,k) = \sum_m \frac{1}{m!} \int dx_{k+1} ... \int dx_{k+m} \otimes \rho_t^{[m]}(1,...,k+m) \prod_{i=k+1}^{k+m} D(1,...,k;i). \tag{4.3}$$

Here the function $D(1,...,k;i)$ gives the probability that the particle at x_i is connected to *at least one* of the particles at $x_1,...,x_k$. It is given by

$$D(1,...,k;i) = 1 - \prod_{m=1}^{k} [1-p_b(x_{mi})]. \tag{4.4}$$

Also, the function $\rho^{[m]}$ is the conditional distribution function

$$\rho_t^{[m]}(1,...,k+m) = \frac{\rho_t(1,...,k+m)}{\rho_t(1,...,k)}. \tag{4.5}$$

We will perform further calculations only in the case of random sphere percolation. In this case, we have $\rho_t(1,...,n) \equiv \overline{\rho}^n$ for all n and Eq. (4.1) becomes

$$n_c(k,\overline{\rho}) = \int I_1(1,...,k) \times \exp\left[-\overline{\rho} \int dx_i D(1,...,k;i) \right]. \tag{4.6}$$

Expanding the exponential in Eq. (4.6) in powers of $\overline{\rho}$ gives a compact expression for the virial coefficients[3,11] of $n_c(k,\overline{\rho})$. We can use this as a laboratory for examining the analytic behavior of this series and its approximants. As we will see, there are certain similarities between truncations of Eqs. (2.7) and (4.1), even though the former is a Kirkwood–Salsburg, and the latter a Mayer–Montroll expansion.[19]

In Fig. 6, we show the first five partial sums of the virial series for the number of dimers, as developed from Eq. (4.6), compared with the results of computer simulation. Explicitly, these are the partial sums of the series[3]

$$\frac{\langle n_c \rangle}{\overline{\rho}} = 4\eta - 49\eta^2 + 302.22\eta^3 - 1250.51\eta^4 + O(\eta^5). \tag{4.7}$$

Several questions suggest themselves:

(1) Are truncations of this virial series alternately upper and lower bounds for the actual cluster densities $n_c(k,\overline{\rho})$? The answer for $k=2$ is empirically yes; however, for general k, the answer is not known. Actually, one cannot yet answer even the weaker question of whether truncations of the virial series for $n_c(\overline{\rho})$, the complete cluster density, form bounds on this quantity. Although this question is analogous, for random sphere percolation, to one answered in the affirmative by Penrose[22] for thermal hard spheres, its answer remains elusive. We discuss this matter further in Sec. VI.

(2) Do the bounds, shown in Fig. 6, improve monotonically? The answer, given empirically, is no; however, one must carefully examine the data at high densities to determine this fact. It is not clear why the nonmonotone behavior of the bounds is much less manifest in this case than, for example, in Fig. 1. The structure of Eq. (4.6) does, however, suggest a simple explanation for the lack of

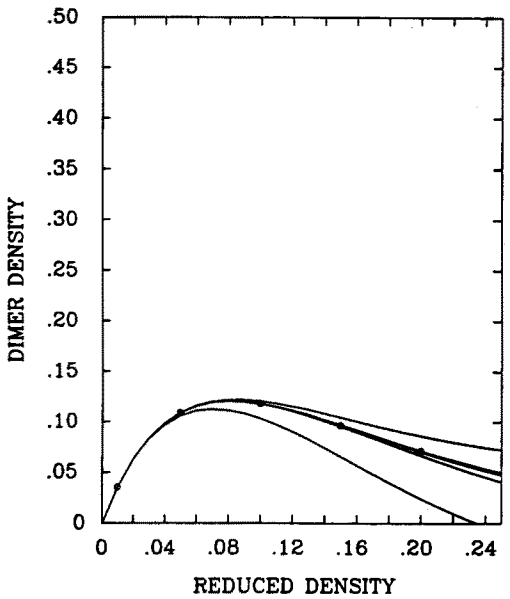

FIG. 6. Successive truncations of the virial series (4.7) for the dimer density, as given by the Mayer–Montroll series (4.6). At low densities, successive truncations alternately form upper and lower bounds of increasing quality, as shown here. This behavior does not persist at very high density; however, compare this figure to Fig. 1.

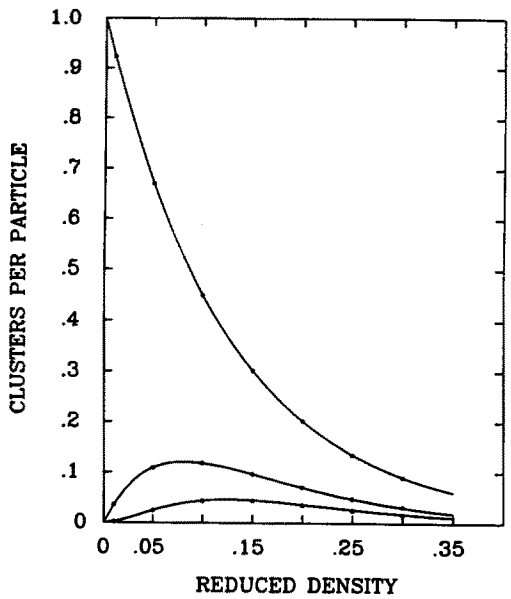

FIG. 7. From top to bottom, density per particle of monomers, dimers, and trimers, in 3D. Curves are analytic formulas; data points are from computer simulation, which can be seen to be in excellent agreement with the exact results. These quantities are needed for the bounds shown in Fig. 9; the agreement between theory and simulation serves to show the high accuracy of the latter.

monotone behavior. Performing a virial expansion of Eq. (4.6) requires expanding an exponential of a negative quantity. The absolute magnitude of the terms in the Taylor expansion of $\exp[-\overline{\rho}V]$ in powers of $\overline{\rho}$ will decrease only after the nth term, where $n \sim \overline{\rho}V$.

V. ENUMERATION BOUNDS FOR THE CLUSTER DENSITY

In this section, we enumerate, for random sphere percolation, the density of monomers, dimers, and trimers, both in two and three dimensions. The calculations, which are carried out either analytically, or using direct numerical integration, serve two purposes. First, they give the first examples of a new class of bounds, which we call enumeration bounds. Second, they serve as input to a study of surface tension in percolation models, which is now under way.[24]

The density, for random sphere percolation, of k mers, is given by Eq. (4.6). The expressions, in two and three dimensions, for dimers and trimers can be reduced, respectively, to single and triple integrations, respectively, over bounded domains. The resulting cluster densities are compared to the results of simulation, for two and three dimensions, in Figs. 7 and 8, respectively. The excellent agreement gives another validation of the method of image boundary conditions described in Ref. 17. The successive sums of these cluster densities give lower bounds on the total cluster density $n_c(\overline{\rho})$, which we call enumeration bounds. The first three such bounds are shown in Fig. 9. However, considering that the sum including trimers, gives the first three virial coefficients exactly, the results for intermediate densities are somewhat disappointing.

We evaluated the quality of this last bound mindful of the fact that many techniques for approximating the transport coefficients of composite materials, e.g., the multiple scattering expansion, are available only for materials of one phase containing nonoverlapping inclusions of another phase. Percolation clusters are nonoverlapping (by definition). Also, one has fairly extensive information about cluster distributions. Thus it is very tempting to describe the well-studied overlapping sphere models[20] of composite media in terms of nonoverlapping inclusions having the

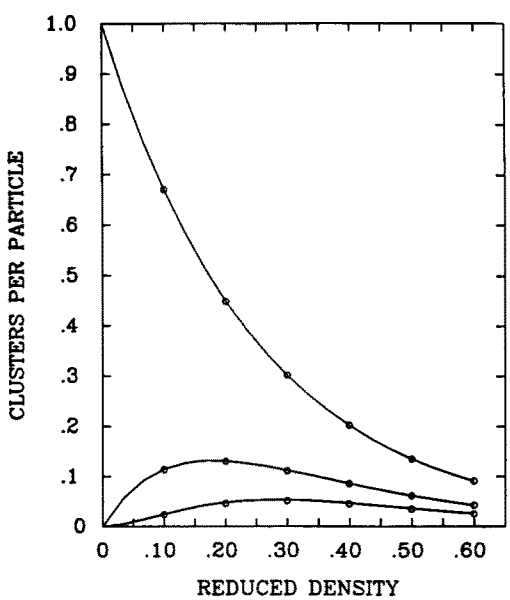

FIG. 8. Same as Fig. 7, but for 2D percolation.

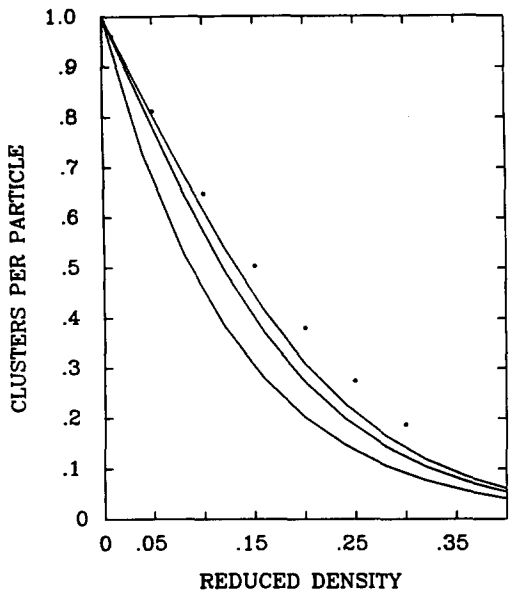

FIG. 9. First three enumerative bounds for full cluster density $\langle n_c \rangle / \overline{\rho}$. Top curve includes monomers, dimers, and trimers. We see that these lower bounds are tight only at low densities.

statistical geometry of the percolation clusters studied in this paper. Experience gained here suggests that naive efforts of this kind might require very extensive enumeration.

VI. CONCLUSIONS

The Kirkwood–Salsburg equations for percolation give formally exact relations that hold for large classes of continuum percolation models. These bounding procedures provide valuable constraints on any approximation scheme. These bounds do not converge rapidly for high densities. However, averaging successive pairs of upper and lower bounds is shown to give remarkably good approximations to our simulation results.

The analytic formulas for the density of small clusters are confirmed in detail by our simulations, thus demonstrating the accuracy of the simulation method used. However, the enumerative bounds formed by summing these are not close approximations even at intermediate densities.

The scaled-particle theory approximations to $\langle n_c \rangle / \overline{\rho}$ match our simulation results very closely except for those of lowest order, both in two and three dimensions. It is obviously worth exploiting this approximation method further, to obtain, for example, the two-point connectedness function and the mean cluster size. The former can be obtained directly by extending the methods of Ref. 25; the latter is then given by a volume integration.[11]

Finally, we investigated two approximation schemes whose analytic status is unclear, the Mayer–Montroll equations and the truncated virial series. Both give sequences of bounds on the cluster density which appear to converge quite well at low and intermediate density. Truncations of the virial series, in particular, converge very well at all densities. These are shown in Fig. 10. They also seem to give the tightest known bounds on $\langle n_c \rangle / \overline{\rho}$. It is of substantial value to further research in percolation theory to substantiate these bounding properties analytically (or to find the class of models for which they break down). Understanding which approximations hold for these models is essential to any attempt to incorporate percolation into realistic theories of disordered materials.

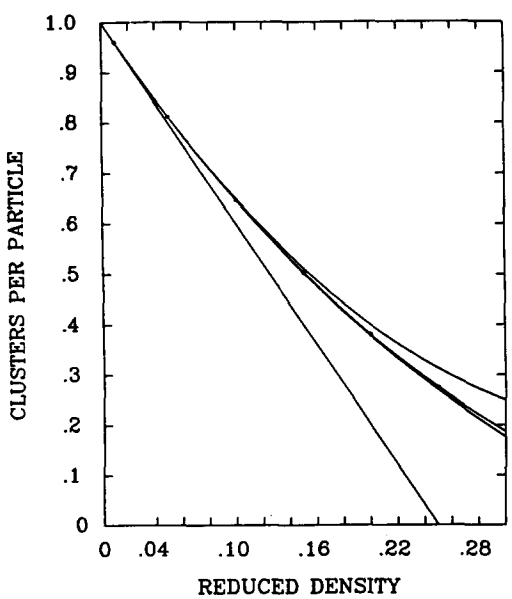

FIG. 10. Partial sums for the virial series for $\langle n_c \rangle / \overline{\rho}$. These give, de facto, extremely tight bounds. Such truncations may, in general, give upper and lower bounds, but this is unproven.

ACKNOWLEDGMENTS

J.G. thanks the Office of Naval Research and G.S. thanks the National Science Foundation for their generous support of our research. Two of us (I.C.K. and S.T.) gratefully acknowledge the support of the Office of Basic Energy Sciences, U.S. Department of Energy, under Grant No. DE-FG05-86ER13582.

APPENDIX A: CALCULATION OF EXACT CLUSTER NUMBERS FOR RANDOM PERCOLATION

In this Appendix, we briefly describe the calculation of the average numbers of percolation clusters of fixed size.

For a general correlated percolation model, the mean number of clusters of fixed size is given by a virial series of Mayer type which has been described.[3] In the specific case of random sphere percolation, one can make use of closed form expressions for the cluster numbers. We describe these in general, but give explicit expressions only for the case of trimers.

If the centers of particles are distributed at random in a volume V with density ρ, the probability that the volume will be empty of them is given by $\exp[-\rho V]$. Using this fact, we can write an expression for the average number of clusters containing exactly s particles

$$n_s = \int dx_{12} \ldots \int dx_{1s} \exp[-\rho V_U]. \tag{A1}$$

Here the integrations are over all sets of pairwise separations such that the s particles form a cluster. The union volume V_U of exclusion spheres surrounding each of the s particles in a cluster must be empty of other particle centers in order that the cluster not contain more than s particles; this accounts for the exponential factor. For trimers in three dimensions, one has the explicit expression

$$n_3=8\pi^2\rho^3\int_0^a r^2\,dr\int_r^a s^2\,ds\int_{-1}^{(r/2s)} d(\cos\theta)\times\exp[-\rho V_U]. \tag{A2}$$

Here θ is the angle between the vector joining particles 1 and 2, and the vector joining particles 2 and 3. The above choice of integration variables is quite efficient in three dimensions, but cannot be used in two dimensions because the corresponding volume element is singular in that case. In two dimensions we have instead

$$n_s=4\pi\rho^3\int_0^a dr\int_r^a ds\int_s^{r+s} dt\,R\exp[-\rho V_U]. \tag{A3}$$

Here R is defined by

$$\sin(\theta)=(t/2R) \tag{A4}$$

and r, s, t are the pairwise distances between the atoms of the trimer. The analytic expression for the volume V_U as a function of r, s, t is given in Ref. 28. Analytic expressions are now available[29] for the union volume V_U of any number of equisized exclusion spheres as a function of their pairwise separations. Thus, one's ability to calculate cluster numbers is limited only by the dimensions of the required phase space integrations. Modern vector computers allow a highly efficient use of the Monte Carlo algorithm to evaluate such integrals.

The mean cluster numbers provide a source of data for continuum percolation in many ways complementary to the calculation of virial coefficients. Small changes to the algorithm for these quantities just described allow one to calculate the mean volume and surface area per cluster. The mean volume is obtained by inserting in the integral (A1) a factor of the cluster volume V_c which is obtained from the same formula as that used for the union volume V_U, but with the exclusion sphere radius a replaced by the particle radius $(a/2)$. The mean surface per cluster is obtained by taking a numerical derivative of the mean volume with respect to the particle radius. This is done by calculating Eq. (A1) with two slightly different values of particle radius, a and $a+\epsilon$, subtracting and dividing by ϵ. The last quantity is presently being used[24] to evaluate the quality of approximate expressions for the surface tension[15] in continuum percolation.

APPENDIX B: FOURTH-ORDER KIRKWOOD–SALSBURG BOUNDS ON THE MEAN CLUSTER NUMBER

In order to better understand the trends in the series (2.9)–(2.12) of bounds of Kirkwood–Salsburg type for $\langle n_c\rangle/\overline{\rho}$, we calculate the fourth-order upper and lower bounds of this type. This is done by eliminating the connectedness functions from Eq. (2.8), using Eq. (2.7), treating exactly terms of order $O(\overline{\rho}^4)$ and approximating higher-order terms so as to preserve bounding properties. The resulting fourth-order bounds are

$$\langle n_c\rangle\geqslant\overline{\rho}-\tfrac{1}{2}\overline{\rho}^2A_2+\tfrac{1}{6}\overline{\rho}^3A_3+\tfrac{1}{24}\overline{\rho}^4C_4+\tfrac{1}{5}\overline{\rho}^5D_5 \tag{B1}$$

and

$$\langle n_c\rangle\leqslant\overline{\rho}-\tfrac{1}{2}\overline{\rho}^2A_2+\tfrac{1}{6}\overline{\rho}^3A_3+\tfrac{1}{24}\overline{\rho}^4C_4+\tfrac{1}{5}\overline{\rho}^5E_5, \tag{B2}$$

where C_4 is the exact virial coefficient for sphere percolation[3,11]

$$C_4=3I_4^{(4)}-6I_5^{(4)}+2I_6^{(4)} \tag{B3}$$

and the remainder terms are given by

$$D_5=-\tfrac{5}{4}A_2^4+\tfrac{11}{4}A_2^3A_3+\tfrac{1}{3}A_2I_5^{(4)}-\tfrac{7}{3}A_2I_6^{(4)}+A_2I_6^{(4)}-\tfrac{2}{3}I_{6a}^{(5)}+\tfrac{2}{3}I_{7a}^{(5)}+\tfrac{1}{3}I_{7b}^{(5)}+\tfrac{1}{3}I_{8b}^{(5)}, \tag{B4}$$

$$E_5=\tfrac{25}{24}A_2^4-2A_2^2A_3-\tfrac{1}{2}A_2I_4^{(4)}+2A_2I_5^{(4)}-\tfrac{1}{2}I_6^{(4)}. \tag{B5}$$

In the above, the $I^{(n)}$ represent the absolute values of the standard Mayer integrals for hard spheres. We follow the terminology of Ref. 30 for them: $I_{6a}^{(5)}$, for example, represents the first cluster integral (in their tabulation) with five vertices and six bonds. It should be noted that bonds in our graphs represent the function $p_b(x)$ given by Eq. (2.2); since this quantity is positive definite, our expressions $I^{(n)}$ are actually the absolute values of the standard Mayer integrals.

APPENDIX C: DERIVATION OF A DIFFERENTIAL EQUATION FOR THE MEAN CLUSTER NUMBER

In this Appendix, we will derive and solve the differential equation for $\langle n_c\rangle$ associated with the scaled-particle approximation scheme (A4).

We assume the form (3.7) for $G(\lambda,\overline{\rho})=g_b(\lambda,\lambda)$, retaining four nonzero terms. Thus,

$$G(y,t)=A_0+\frac{A_1}{y}+\frac{A_2}{y^2}+\frac{A_4}{y^4}. \tag{C1}$$

The coefficient A_3 can be shown to be identically zero in general.[15] The osmotic pressure equation for percolation (3.6) then gives

$$\langle n_c\rangle/\overline{\rho}=A_0. \tag{C2}$$

The constraint equations given by fixing the values of the function G and its derivative at $y=\frac{1}{2}$ can be shown to be[15]

$$G\Big|_{y=1/2}=e^{-t}, \tag{C3}$$

$$\frac{dG}{dy}\Big|_{y=1/2}=-6te^{-t}. \tag{C4}$$

The charging relation (3.4) can be rewritten, using Eq. (C2) on the left-hand side, as

$$\frac{dG}{dt}+G=e^{-t}-24t\int_{1/2}^{1}G(y,t)y^2\,dy. \tag{C5}$$

Finally, the virial theorem (2.17) becomes

$$\frac{d}{dt}\left(\frac{\langle n_c\rangle}{\bar{\rho}}\right)=-4G(y=1,t). \tag{C6}$$

Substituting Eq. (C1) into Eqs. (C3)–(C6) gives

$$A_0+2A_1+4A_2+16A_4=e^{-t}, \tag{C7}$$

$$4A_1+16A_2+128A_4=6te^{-t}, \tag{C8}$$

$$tA_0'+A_0=e^{-t}-24t[C_0A_0+C_1A_1+C_2A_2+C_4A_4], \tag{C9}$$

$$A_0'=-4[A_0+A_1+A_2+A_4]. \tag{C10}$$

Here the prime indicates a t derivative. The constants C_n are given by

$$C_n=\int_{1/2}^{1}y^{2-n}\,dy. \tag{C11}$$

Combining Eqs. (C7)–(C10) and eliminating the variables A_1-A_4 gives for A_0:

$$-\tfrac{1}{5}tA_0'+A_0=[\tfrac{9}{10}t^2-\tfrac{12}{5}t+1]e^{-t}+\tfrac{1}{5}tA_0. \tag{C12}$$

By inspection, we find the solution

$$A_0=\frac{\langle n_c\rangle}{\bar{\rho}}=[\tfrac{3}{2}t^2-3t+1]e^{-t} \tag{C13}$$

which approaches unity as the density t approaches zero. This approximation is shown as the lowermost dotted curve in Fig. 4. It is found[15] that Eq. (C13) also results if the set of constraints is simplified so as to eliminate either the charging equation or the osmotic pressure equation and set the trial parameter A_4 to zero.

[1] The literature is rapidly growing. We give only some representative references that include those of particular relevance to the approaches discussed here.
[2] A. Coniglio, U. de Angelis, and A. Forlani, J. Phys. A **10**, 1123 (1977).
[3] S. Haan and R. Zwanzig, J. Phys. A **10**, 1547 (1977).
[4] G. Stell, J. Phys. A **17**, 1855 (1984); Y. Chiew, G. Stell, and E. Glandt, J. Chem. Phys. **83**, 761 (1985).
[5] Y. Chiew and E. Glandt, J. Phys. A **16**, 2599 (1983); J. Xu and G. Stell, J. Chem. Phys. **89**, 1101 (1988).
[6] T. L. Hill, *Statistical Mechanics* (McGraw–Hill, New York, 1956).
[7] C. Fortuin and P. W. Kastelyn, J. Phys. Soc. Jpn. (Supp.) **26**, 11 (1969).
[8] E. Sevick, P. Monson, and J. M. Ottino, J. Chem. Phys. **88**, 1198 (1988); N. A. Seaton and E. D. Glandt, *ibid.* **86**, 4668 (1987).
[9] L. Fanti, E. Glandt, and Y. Chiew, J. Chem. Phys. **89**, 1055 (1988).
[10] I. Webman, J. Jortner, and M. Cohen, Phys. Rev. B **11**, 2885 (1975).
[11] J. Given and G. Stell, Physica A **161**, 152 (1989).
[12] W. Klein, Phys. Rev. B **26**, 2677 (1984).
[13] J. Given and W. Klein, J. Chem. Phys. **90**, 1116 (1989); J. Given, *ibid.* **90**, 1333 (1989).
[14] J. Given and G. Stell, J. Stat. Phys. **59**, 981 (1990).
[15] J. Given and G. Stell, S.U.N.Y. Stony Brook C.E.A.S. Report 538, February 1989; J. Chem. Phys. **92**, 4433 (1990).
[16] S. Torquato, and S. B. Lee, J. Chem. Phys. **91**, 1173 (1989); S. B. Lee and S. Torquato, *ibid.* **89**, 6427 (1988).
[17] J. Hoshen and R. Kopelman, Phys. Rev. B **28**, 5323 (1983).
[18] B. Widom and J. Rowlinson, J. Chem. Phys. **52**, 1670 (1970).
[19] G. Stell, in *The Wonderful World of Stochastics*, edited by M. F. Schlesinger and G. H. Weiss (North Holland, Amsterdam, 1985).
[20] S. Torquato and G. Stell, J. Chem. Phys. **77**, 2071 (1982).
[21] J. Lebowitz and J. Percus, J. Math. Phys. **4**, 1495 (1963).
[22] J. Groeneveld, Phys. Lett. **3**, 50 (1962); O. Penrose, J. Math. Phys. **4**, 1312 (1963); D. Ruelle, Ann. Phys. (N.Y.) **25**, 109 (1963).
[23] J. Mayer and E. Montroll, J. Chem. Phys. **9**, 2 (1941).
[24] J. Given, I. C. Kim, S. Torquato, and G. Stell (to be published).
[25] H. Reiss and R. V. Casberg, J. Chem. Phys. **61**, 1107 (1974).
[26] G. Stell, "Statistical Mechanics Applied to Random Media Problems", AMS–SIAM Proceedings of the Workshop on Random Media (to be published).
[27] H. Reiss, H. Frisch, and J. Lebowitz, J. Chem. Phys. **31**, 369 (1959).
[28] M. J. D. Powell, Mol. Phys. **7**, 591 (1964).
[29] K. W. Kratky, J. Stat. Phys. **25**, 619 (1981); see also K. D. Gibson and H. A. Scheraga, Mol. Phys. **62**, 1247 (1987), and references therein.
[30] J. S. Rowlinson, Proc. R. Soc. London Ser. A **279**, 147 (1964); see also J. E. Kilpatrick, Adv. Chem. Phys. **20**, 39 (1971).